KONA Powder and Particle Journal

KONA Powder and Particle Journal No. 42 (2025) 213–226/https://doi.org/10.14356/kona.2025005 Review Paper

Recent Advances in Nitride Composites for Effective Removal of Organic Dyes in Wastewater Treatment†

Wenjea J. Tseng

Department of Materials Science and Engineering, National Chung Hsing University, Taiwan

The presence of organic dyes from industrial effluents has caused growing environmental and human health concerns. Various remediation methods and materials are available to minimize the environmental impact and ensure safe drinking water. Nitride composite particles have recently emerged as one of the promising materials for the efficient and selective removal of toxic and hazardous substances (including organic and inorganic compounds) from industrial wastewater. This review summarizes recent advances in the disposal of organic dyed wastewater using advanced nitride composite particles, including graphitic carbon nitride-based nanocomposites, boron nitride composites, and two-dimensional transition metal nitrides. The selection of appropriate materials remains largely a trial-and-error approach at present. This review highlights multiple dye-removal mechanisms, such as photocatalytic degradation, dye-sorption behavior, and computational analysis, to aid the material selection and shed light on the interactions between organic dye contaminants and nitride composites.

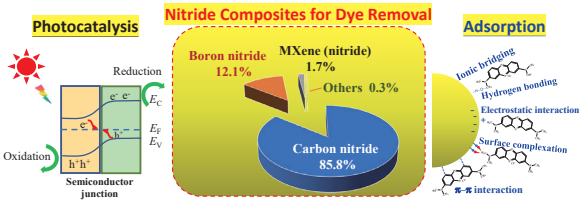

Keywords: nitride, composite, dye removal, adsorption, photocatalysis

1. Introduction

Water is an essential resource for life on Earth, and its quality is vital for the health and well-being of both humans and the environment. According to a United Nations report, an estimated 47 % of the world's population will face a clean-water shortage by 2030 (Connor, 2015). Population growth, urbanization, and anthropogenic activities contribute to the increasing global water demand by 50 % by the year 2050 (Connor, 2015). Wastewater, the water discharged after use in households, industries, and agriculture, has already become a significant source of pollution that might have severe consequences for the environment and human health. Failure to treat the wastewater properly may harm public health since the untreated wastewater might contain harmful microorganisms, viruses, and chemicals that can cause diseases (Dickin et al., 2016; Adegoke et al., 2018; Choudri and Charabi, 2019). Removal of these harmful contaminants reduces the risk of waterborne illnesses. In addition, eutrophic wastewater may contain nutrients like nitrogen and phosphorus that can cause excessive algae growth in water bodies, leading to oxygen depletion and fish kills (Lapointe et al., 2015; Preisner et al., 2020, 2021). Toxic chemicals in untreated wastewater may also harm aquatic life, damage ecosystems, and enter the food chain (Al-Tohamy et al., 2022; Hamidian et al., 2021; Islam et al., 2021; Saravanan et al., 2021). Treating wastewater protects the environment and helps conserve water resources by reducing the demand for freshwater resources, ensuring sufficient water to meet the needs of people and industries.

Textile and pigment industries significantly contribute to the global economy and environmental pollution. The global market of dyes and pigments was valued at USD 38.2 billion in 2022 and may grow at a compound annual growth rate of 5.3 % from 2023 to 2030 (Market Analysis Report, 2023). The market forecast indicates a growing demand for colorants worldwide, which consume over a million tons of dyes annually (Singh and Arora, 2011; Al-Tohamy et al., 2022). Using organic dyes in textile and pigment industries can thus have negative environmental and health impacts if not properly managed (Lellis et al., 2019). Industries must adopt sustainable and responsible practices, such as eco-friendly dyes and proper wastewater treatment, to minimize environmental and health impacts.

More than 100,000 commercial dyes have been reported on the market (Yagub et al., 2014). Some of the most common organic dyes used in textile industries include: i) reactive dyes for their color fastness and ability to bond with a wide range of fabric fibers, ii) acid dyes for their bright and vibrant colors to wool, silk, and nylon fibers in fabrics, iii) disperse dyes for their ability to bond with the synthetic fibers with color fastness, iv) direct dyes for dyeing cellulosic fibers with their ease of use and affordability, v) vat dyes for their excellent color fastness to stain cotton, rayon, and other cellulosic fibers, and vi) sulfur dyes for dyeing

† Received 3 July 2023; Accepted 23 August 2023
J-STAGE Advance published online 17 March 2024
Add: Taichung 402, Taiwan
E-mail: wenjea@dragon.nchu.edu.tw
TEL: +886-4-22870720 FAX: +886-4-22857017

cellulosic fibers such as cotton and rayon with affordable price and good color fastness (Bechtold et al., 2007; Degano et al., 2009; Zollinger, 2003). Similarly, the pigment industry uses a wide range of organic dyes to produce colorants, including: i) azo dyes consisting of the azo group (–N=N–) as the chromophore for their bright and vibrant colors, ii) phthalocyanine dyes for their blue and green hues, iii) anthraquinone dyes for their lightfastness and color fastness, iv) quinacridone dyes for their bright and vivid colors, v) indigo dyes for their blue color in the production of denim, and vi) perylene dyes for their lightfastness and good color fastness (Zollinger, 2003).

The vast compositional diversity and structural complexity of the organic colorants used in the textile and pigment industries inevitably make complete dye removal an insurmountable task in wastewater treatment. Various methods are available for treating synthetic dyes, e.g., physical, chemical, and biological approaches (Al-Tohamy et al., 2022; Forgacs et al., 2004; Martıńez-Huitle and Brillas, 2009; Singh and Arora, 2011; Yaseen and Sholz, 2019). **Table 1** highlights the advantages and disadvantages of the most frequently used dye removal techniques. Having a method that can effectively remove various types of dyes is challenging. Still, the method's effectiveness depends primarily on specific dyes present in the wastewater and the characteristics of the method used. Some processes may be more effective for removing specific dyes, depending mainly on their chemical properties, such as their molecular structure, solubility, and reactivity. In practice, a combination of methods may become necessary to achieve the desired level of dye removal.

For the materials used in organic dye removal, there have been some excellent reviews covering a wealth of natural and synthetic materials for wastewater remediation (Forgacs et al., 2004; Islam et al., 2021; Martıńez-Huitle and Brillas, 2009; Singh and Arora, 2011; Yagub et al., 2014). Some commonly used natural materials include activated carbon, clay minerals, zeolite, agricultural by-products (e.g., husk, leaf, sawdust, and peel from the plant, chitosan made from the shell of crustaceans), and industrial by-products (e.g., mud, fly ash). Many of these materials purify the dyed wastewater by adsorption (Yagub et al., 2014). Materials possessing high porosity and large surface area are highly desirable as effective sorbents and photocatalysts for selective dye removal. With the rapid development of nanostructured synthetic materials in recent decades, nitride composite particles have emerged as promising materials for efficiently removing organic dye pollutants from industrial wastewater. **Fig. 1a** shows a chronological evolution of reported scientific papers on

Table 1 Pros and cons of methods used for organic dye removal.

Methods	Pros	Cons
Physical Approach		
(i) Adsorption	Applicable for treating a wide variety of dyes	Needs regular adsorbent replenishment and sludge cleaning
(ii) Ion exchange	Able to handle a large volume of wastewater; requires no chemicals	Impractical to remove some dyes and contaminants that are not ionizable
(iii) Membrane filtration	Applicable for treating a wide variety of dyes efficiently in large volumes	Needs periodic replacement of fouled membrane; often requires energy supply to maintain the pressure needed for filtration
Chemical Treatment		
(i) Coagulation and flocculation	Effective in removing various dyes in large volumes	Often pH sensitive; requires the use of chemicals, and generates sludges
(ii) Advanced chemical oxidation	Removes target dyes selectively in large volumes by the formation of $OH^{\bullet}$	Requires the use of chemicals and may generate harmful by-products; may require longer reaction time
(iii) Electrochemical method	Fast and effective at removing a wide range of both synthetic and natural dyes; able to use renewable energy sources	High electricity consumption; requires specialized knowledge in system design and operation
Biological Approach		
(i) Enzyme-based method	Selective dye removal with energy-saving and environmentally friendly features; less sludge formation	Limited effectiveness and slow processing for large volumes
(ii) Microbial method	Natural and low cost; may have a high removal efficiency for certain types of dyes	Limited effectiveness and slow processing for large volumes; may be sensitive to environmental conditions

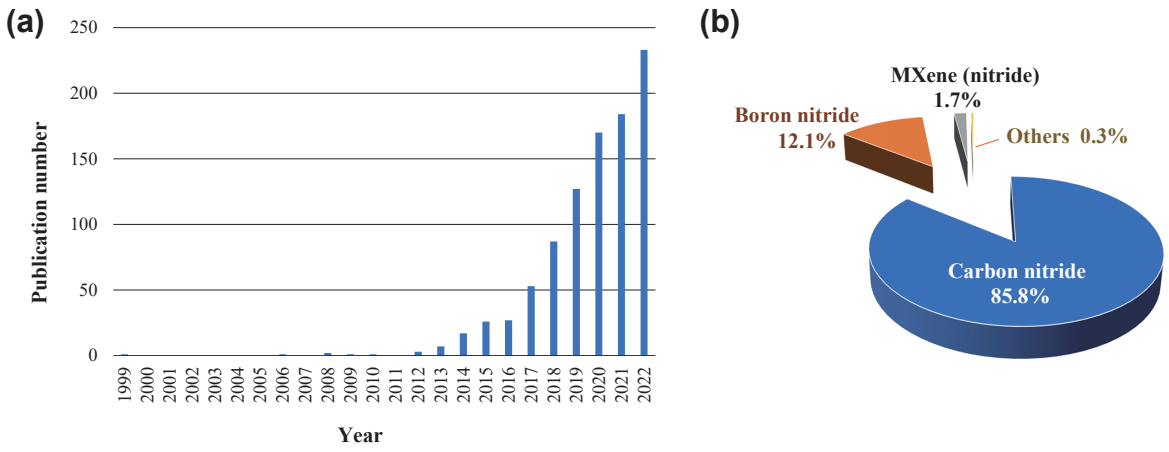

Fig. 1 **(a)** Publication numbers on nitrides in chronological order for dye removal (Data from Web of Science search using keywords of "nitride", "dye", and "rem*"). **(b)** Publications sorted by materials illustrating the weighted fractions.

nitrides for dye removal. Intensive research has been directed toward wastewater treatment using nitride nanomaterials since about a decade ago. This result is attributable to the emergence of two-dimensional (2D) semiconducting graphitic carbon nitride (g-C_3N_4) nanosheets and their three-dimensional (3D) porous counterparts. The g-C_3N_4 nanostructures show promise of harnessing visible light for the photocatalytic degradation of organic dyes together with adsorption capability toward selective organic pollutants (Acharya and Parida, 2020; Hu et al., 2019; Lam et al., 2016; Santoso et al., 2020). The fact that g-C_3N_4 gained significant attention is demonstrated by the publication of the first highly cited article in 2012 (Cui et al., 2012) from the Web of Science search. **Fig. 1b** further illustrates the prevalent dominance of the g-C_3N_4 in published nitride-related water-remediation papers with a substantial 85.8 %. Boron nitride (BN) and transition metal carbide/nitride (MXene) with 2D layered structures follow in the distant second and third positions of 12.1 % and 1.7 %, respectively.

While literature reviews have extensively focused on carbon nitride-based nanomaterials, we envision that a more comprehensive understanding of nitride-based nanocomposites will significantly contribute to developing next-generation multi-purpose dye-removal solutions. Considering their potential use in wastewater treatment, this review aims to cover the recent progress in material design, fabrication method, and dye-removal performance of various nitride nanocomposites. Selecting appropriate dye-removal materials largely remains a trial-and-error approach at present. The review highlights multiple dye-removal mechanisms, such as the photocatalytic degradation and dye-sorption behavior of the composite nitride nanoparticles, together with computational analyses that show promises of shedding light on the nature of interactions between organic dye contaminants and nitrides. Finally, some future perspectives will be addressed.

2. g-C_3N_4-based nanocomposites

Carbon nitride is a class of compound materials composed of carbon and nitrogen atoms with various structures and properties. Different allotropes exist for the carbon nitride, including alpha, beta, cubic, pseudo-cubic, amorphous, and g-C_3N_4 (Aspera et al., 2010; Wang et al., 2017). Among them, g-C_3N_4 possesses a repeating unit of stacked carbon atoms and nitrogen-rich functional groups arranged in a honeycomb-like structure resembling graphite. The unique combination of features includes an n-type semiconductor with a tunable optical bandgap around 2.7 eV suitable for harnessing visible light, excellent chemical and thermal stability because of the covalent nature of the carbon–nitrogen bonding for use in harsh environments, facile preparation with environmental friendliness, a metal-free chemical attribute with earth abundance, and low cytotoxicity (Ahmadi et al., 2023; Dong et al., 2014; Jiang et al., 2017; Teter and Hemley, 1996; Thomas et al., 2008; Xu et al., 2018; Zhao et al., 2015). **Fig. 2** shows the primary tectonic units of g-C_3N_4, which include two major substructures, i.e., triazine and tri-s-triazine (heptazine). The tri-s-triazine-based structure is the most stable allotrope in the ambient environment (Dong et al., 2014; Thomas et al., 2008).

The stacking layer structure in the g-C_3N_4 allotrope consists of the sp^2 hybridization of carbon and nitrogen heteroatoms with features of tunable interlayer spacing through changing the localization of electrons and the binding energy between neighboring layers. The structure generates the π-conjugated graphitic planes with tunable positions of the highest occupied molecular orbital (HOMO) and the lowest unoccupied molecular orbital (LUMO) as a semiconducting photocatalyst for the purification of dye-contaminated wastewater (Zhao et al., 2021).

Intrinsic drawbacks, such as insufficient absorption of light energy, low surface area, and fast recombination of photogenerated electrons and holes, suppress the

photocatalytic efficiency of bulk g-C_3N_4 photocatalyst. The photoelectronic conversion of g-C_3N_4 would enhance substantially by increasing the nitrogen content, as the presence of nitrogen atoms impacts the spin density and charge distribution of the carbon atoms. This creates active sites on the surface to remove organic dyes and pigments efficiently under light illuminations (Ahmadi et al., 2023). Various strategies have been explored to overcome the shortcomings of g-C_3N_4 photocatalysts, including doping of metal or non-metal elements, creation of semiconducting junctions with suitable band structures at the interface, morphological control, and defect-modulating engineering (Acharya and Parida, 2020; Kumar et al., 2022; Luo et al., 2023; Xu et al., 2018). The construction of heterojunction involving g-C_3N_4 nanosheet composite with a semiconductor having a matched band-edge potential is promising for enhancing the separation efficiency of photoinduced charge carriers together with synergistically enriching light-harvest ability. For example, **Fig. 3a** shows a hypothetical charge-transfer route when two coupled semiconductor photocatalysts display the staggered band structure at the interface. The photogenerated electrons are thought to flow from photocatalyst 2 to photocatalyst 1 under light irradiation, while the opposite is true for the photogenerated holes, facilitating the separation of charge carriers. The idealized recombination suppression occurs at the expense of reduced redox activity for photocatalysis. In addition, the electrostatic repulsion between the like charges may inhibit the continuous accumulation of charge carriers from transferring (Xu et al., 2020). In this regard, the Z-scheme photocatalyst with a suitable intermediate couple between two contacting semiconductors provides a promising alternative to facilitate the charge separation while retaining a strong redox ability in **Fig. 3b** (Kudo and Miseki, 2009; Li et al., 2016). In a typical all-solid-state Z-scheme photocatalyst, a solid conductor is used to replace the shuttle-redox ion pairs in traditional Z-scheme for imparting the transfer of charge carriers at the semiconductor junction. The evolvement toward direct Z-scheme later occurs, as demonstrated in a g-C_3N_4/TiO_2 composite photocatalyst by Yu et al. in 2013, which does not require an intermediate electron mediator to attain a robust photocatalytic capability. They have shown that the disparity in the work functions of g-C_3N_4 and TiO_2 renders the formation of an internal electric field at the junction so that an inherent actuating force takes place to replace the intermediate electron mediator. This development leads to a step-scheme (known as the S-scheme) heterojunction involving a

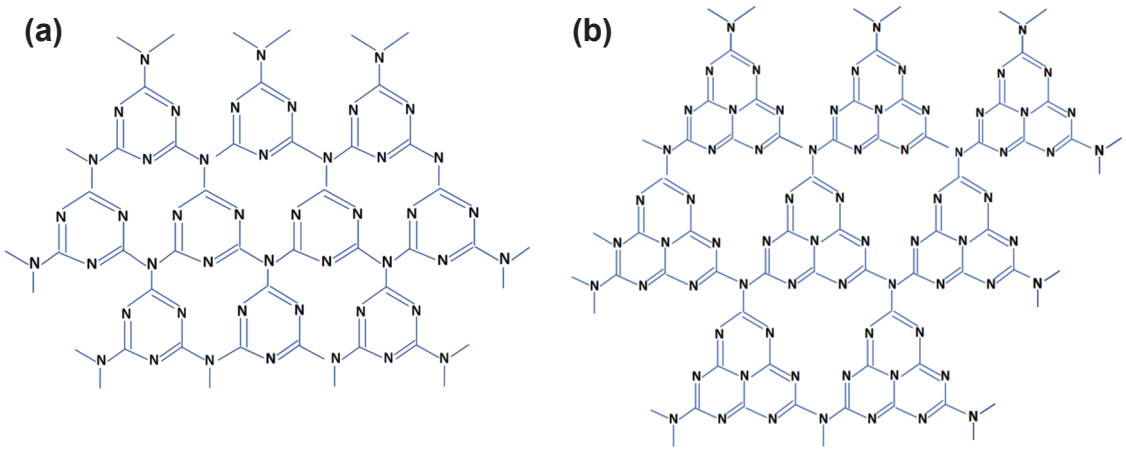

Fig. 2 Primary tectonic units of **(a)** triazine and **(b)** tri-s-triazine for g-C_3N_4 allotropes.

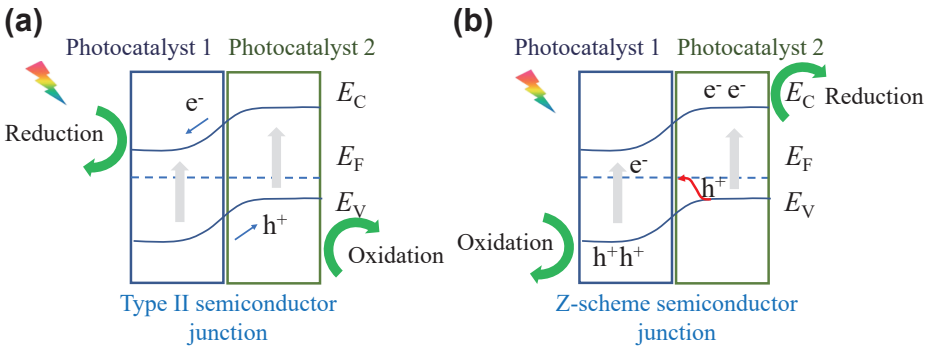

Fig. 3 Examples of possible charge-transfer routes at the semiconductor junction for **(a)** Type II (staggered gap) and **(b)** direct Z-scheme/S-scheme heterojunctions.

semiconducting couple containing an oxidation photocatalyst (i.e., photocatalyst 1 in **Fig. 3b**) and a reduction counterpart (i.e., photocatalyst 2 in **Fig. 3b**) to form the staggered band structure with a charge-transfer route resembling that of the Z-scheme while remaining a strong redox capability (Xu et al., 2020; Zhang et al., 2022).

Table 2 lists selected examples of dye-removal performance using g-C_3N_4 nanocomposite photocatalysts in dyed water treatment. Various g-C_3N_4 nanocomposites have been examined for the photocatalytic removal of organic dye pollutants. In view of the literature in **Table 2**, we may conclude that heterojunction with a suitable band alignment allows simultaneously the creation of active sites and efficient separation of photoinduced charge carriers for facilitating dye decomposition under light illuminations.

The pursuit of highly efficient g-C_3N_4-based composite photocatalyst depends critically on the synthesis process since the attainment of mesoporous 2D g-C_3N_4-based nanocomposites with high surface area, tailored pore size and pore shape is advantageous in providing active chemical sites on the surface for the selective photodegradation of organic dyes. Appropriate defects residing at the surface are potentially beneficial for enhanced photocatalysis (Acharya and Parida, 2020; Darkwah and Ao, 2018; Ismael et al., 2019; Zhao et al., 2018; Zhu et al., 2014). Various nitrogen-rich organic precursors containing C–N bonding structure without direct C–C bonding have been used as the precursor compound for the g-C_3N_4 synthesis, e.g., cyanamide, dicyandiamide, melamine, thiourea, urea, or their mixtures, via the polycondensation route. A low surface area often results due mainly to the formation of a layered graphitic structure. Two main process strategies have been proposed to resolve this shortcoming, i.e., the hard- and soft-templating routes for the g-C_3N_4 synthesis. The prepared g-C_3N_4 nanosheets often favor depositing on a template with a high surface area. **Table 3** lists the differences between the hard- and soft-templating methods. The hard-templating approach involves using a sacrificial hard template, such as mesoporous silica, for the impregnation with a precursor compound (Groenewolt and Antonietti, 2005; Wang et al., 2009). The removal of the template by calcination or chemical etching forms g-C_3N_4 with a porous structure that replicates the shape of the template. On the other hand, the soft-templating approach involves using a soft template, such as surfactants or block copolymers, which self-assemble to form a template for the organic precursor (Lu et al., 2014; Yan, 2012). After deposition of the precursor onto the template, the template can be removed by washing or mild calcination, leaving behind g-C_3N_4 with a mesoporous structure that replicates the shape of the template.

A large surface area with a suitable pore structure for allowing organic dye molecules more access to the surface moiety of g-C_3N_4 nanocomposite is one important parameter affecting dye removal in wastewater treatment. Surface characteristics of the mesoporous g-C_3N_4-based nanocomposite are also essential for imparting high activity as an efficient adsorbent. Aspera et al. (2010) have shown that bonding occurs favorably between the hydrogen atom of the water molecule and the two-coordinated nitrogen atom of the tri-s-triazine-based g-C_3N_4 with a chemisorption energy of –0.82 eV by *ab initio* density functional theory (DFT) computations. Modwi et al. (2022) verified recently that hydrogen-bonding interactions occur favorably between OH groups of mesoporous MgO/g-C_3N_4 nanocomposite and lone-pair electrons of amine groups of basic fuchsin (BF) dyes, resulting in a pronounced adsorptive uptake selectively.

In addition to the hydrogen bonding, mechanisms involved in the dye adsorption of g-C_3N_4 nanocomposites include electrostatic interaction, π–π interaction, surface complexation, and cation bridge (Chen et al., 2020; Fronczak, 2020). **Table 4** lists selected examples of adsorptive dye removal using g-C_3N_4 nanocomposites in dyed water treatment. The electrostatic interaction occurs preferentially when g-C_3N_4 and dye molecules bear surface charges of different signs in water. Zhu et al. (2015) measured the isoelectric point (IEP) around 4 to 5 for g-C_3N_4 prepared using melamine, thiourea, and urea as the precursor compounds, respectively. The experimentally determined IEP reflects the chemical equilibrium between hydrogen ions, hydroxyl ions, and amine groups on the g-C_3N_4 surface in an aqueous medium. The adsorption activity increases when the negatively charged g-C_3N_4 surface encounters cationic methylene blue (MB) dye molecules at a solution pH more positive than the pH_{IEP}. At the same time, the opposite is true for the anionic methyl orange (MO) dye molecules. The π–π interaction occurs when both g-C_3N_4 and organic dye structures contain aromatic pendant groups, so adsorption occurs via non-covalent bonding. Meng and Nan recently reported the rapid and selective adsorption of organic MB dyes in water using Na and Fe co-doped g-C_3N_4 (Meng and Nan, 2022). The infrared spectra verified the π–π conjugation between MB dyes and g-C_3N_4 adsorbents for selective removal. The conjugation, electrostatic interactions, and hydrogen bonding contribute to the synergistic adsorptive MB removal. The complexation mechanism arises primarily from the metal doping to the g-C_3N_4 structure, which creates binding sites and functional groups that can firmly adhere to the dye molecules by forming surface complexes.

Similarly, the cation-bridge mechanism involves the ion exchange of charged metal compounds in the g-C_3N_4 structure with the ionized cations of the dye molecules. Nnadiekwe et al. (2023) have recently employed DFT computations to examine the adsorption behavior of alkali ions (including Li^+, Na^+, K^+) doped heptazine-based g-C_3N_4 nanocomposites to the cationic MB dyes in water.

Table 2 Selected examples of photocatalytic dye-removal performance using g-C_3N_4 nanocomposites in dyed water treatment.

Catalyst	Dye	Light source	Catalyst dosage (mg)	Dye-removal performance	Reference
g-C_3N_4/WO_3	MB (100 mL, 10 mg·L^{-1})	300 W Xe lamp with 400 nm cutoff filter	100	97 %, 120 min	Huang et al., 2013
g-C_3N_4/BiOI	Rhodamine B (RhB), MB, MO (all 100 mL, 10 mg·L^{-1})	300 W Xe lamp with 400 nm cutoff filter	10–20	ca. 99 %, 50 min for RhB, >95 % for MB and MO	Di et al., 2014
g-C_3N_4/SnO_{2-x}	RhB (100 mL, 10 mg·L^{-1})	350 W Xe lamp with UV and IR cutoff filters	40	ca. 99 %, 60 min	He et al., 2015
g-C_3N_4/reduced graphene oxide (RGO)	MB (100 mL with 1 mL H_2O_2, 5 mg·L^{-1})	500 W Xe lamp	2.5 (membrane) for flow-through dye degradation	>95 %, 150 min	Li et al., 2017
g-C_3N_4/TiO_2 (black)	MO (30 mL, 10 mg·L^{-1})	300 W Xe lamp with 420 nm cutoff filter	30	95 %, 150 min	Shen et al., 2017
g-C_3N_4/BiOCl	4-chlorophenol (an intermediate for dye synthesis, 100 mL, 10 mg·L^{-1})	300 W Xe lamp with 420 nm cutoff filter	50	ca. 95 %, 150 min	Wang et al., 2018
CoAl-LDH/g-C_3N_4/RGO (LDH: Layered double hydroxide)	Congo red (CR)			ca. 95 %, 30 min	Jo and Tonda, 2019
g-C_3N_4/RGO	RhB (40 mL, 5 mg·L^{-1})	300 W Xe lamp with 420 nm cutoff filter	40	>98 %, 30 min	Wei et al., 2019
g-C_3N_4/ZnO/$ZnFe_2O_4$ and g-C_3N_4/ZnO/$CoFe_2O_4$	MO, Malachite green (MG) (150 mL, 10 mg·L^{-1})	10 W LED lamp (400–700 nm)	50	ca. 95 %, 70 min (MG), 140 min (MO)	Chandel et al., 2020
g-C_3N_4/MoS_2	MB (20 mL, 5 ppm)	UV, visible, and sun light	1	98.7 %	Monga et al., 2020
Phosphorus sulfur co-doped g-C_3N_4/BiOBr/Ag/AgCl	Phenol	35 W LED lamp		98 %, 60 min	Raizada et al., 2020
g-C_3N_4/red mud	MB, MG (10 mg·L^{-1})	300 W Xe lamp with 420 nm cutoff filter	50	ca. 95 %, 80 min (MB), 120 min (MG)	Shi et al., 2020
g-C_3N_4/CuI	RhB, MO (150 mL, 10 ppm)	400 W UV, 150 W visible light	150	Up to 98.5 % under UV, and 78.6 % under visible irradiations	Ghanbari and Salavati-Niasari, 2021
Sulfur-doped g-C_3N_4/Ag/ZnO	MB (100 mL, 10 mg·L^{-1})	Sunlight (57–63 Klux)	10	>90 %, 60 min	Iqbal et al., 2021
g-C_3N_4/Ni/ZnO	MB (200 mL, 10 mg·L^{-1})	Sunlight (68–73 Klux)	200	ca. 99 %, 70 min	Qamar et al., 2021
g-C_3N_4/Cd/ZnO	MB (100 mL, 10 mg·L^{-1})	Sunlight	10	>90 %, 90 min	Sher et al., 2021
Fe-doped g-C_3N_4	RhB (50 mL, 10 mg·L^{-1})	Visible light	25	ca. 98.2 %, 60 min	Ding et al., 2022
g-C_3N_4/BiOBr	RhB (25 mL, 20 mg·L^{-1})	300 W Xe lamp with 420 nm cutoff filter	20	87 %, 30 min	Tian et al., 2022

Table 3 Pros and cons of hard- and soft-templating methods used to synthesize mesoporous 2D g-C_3N_4-based nanocomposite.

Methods	Pros	Cons
Hard-templating approach	Reasonable control over pore size and distribution; high stability; easily scaled up for industrial production	The range of pore size is typically limited by the available template materials; time-consuming process; limited flexibility in terms of the variety of pore shapes and structures that can be produced.
Soft-templating approach	High flexibility for a wide range of pore shapes and structures to be produced; relatively fast for the template removal; cost-effective in terms of the soft-template material	Poor control over pore size and distribution; less stable due to the weaker interaction between the carbon nitride and the soft template material; limited scalability

Table 4 Selected examples of g-C_3N_4 nanocomposites for the adsorptive organic dye removal in water treatment.

Adsorbent	Dye	Adsorbent dosage (mg)	Adsorption removal	Reference
Fe-doped g-C_3N_4/graphitized mesoporous carbon	Acid red 73, RhB (50 mg·L^{-1}, H_2O_2 40 mM)	200*	>99 %, 40 min (pH = 6.9)	Ma et al., 2017
g-C_3N_4/red mud	MB, MG (10 mg·L^{-1})	50	ca. 35 %, 30 min (MB), ca. 70 %, 30 min (MG)	Shi et al., 2020
g-C_3N_4/TiO_2	MO (50 mg·L^{-1}, 10 mg·L^{-1})	10	ca. 80 %, 15 min (pH ca. 7)	Wang et al., 2020
g-C_3N_4/TiO_2/GO	MO, MB, CR, RhB (10 mg·L^{-1})	Foam	>97 %	Zhan et al., 2021
g-C_3N_4/MgO	CR, Basic Fuchsin (BF) (25 mL, 50 mg·L^{-1})	10	96 %, 24 h (CR); 99 %, 24 h (BF)	Modwi et al., 2022
Na and Fe co-doped g-C_3N_4	MB (50 mL, 50 mg·L^{-1})	5	ca. 90 %, 5 min (MB, pH = 6.5)	Meng and Nan, 2022

*: Estimated using 250 mL for the dyed solution.

Their calculation shows that the Li^+-doped g-C_3N_4 exhibits the smallest HOMO–LUMO gap and the highest charge potential compared to the K^+ and Na^+ counterparts. The predicted adsorption performance is in an ascending order of K^+-doped g-C_3N_4 < Na^+-doped g-C_3N_4 < Li^+-doped g-C_3N_4, depending mainly on the protonation of the g-C_3N_4 nanosheets.

Although the selected examples of adsorptive dye removal in **Table 4** appear fewer than those of photocatalytic degradation in **Table 2**, it may be interesting to note that organic dye removal often involves photocatalysis and adsorption mechanisms being both operative simultaneously for many g-C_3N_4 nanocomposites in wastewater treatment (Shi et al., 2020). The observation is reasonably justifiable since redox interactions between charge carriers and dye molecules likely favorably occur upon exposure to light irradiation when the organic dye pollutants adsorb on the surface of g-C_3N_4 photocatalysts. Accordingly, organic adsorption and photodegradation may be regarded as an integral interaction route for overall pollutant removal. In this regard, attempts at real-time monitoring of the in-situ adsorption and photodegradation of dye molecules are challenging. Recently, Qin et al. (2021) reported their finding using attenuated total reflectance induced evanescent spectroscopy (ATR-ES). The ATR-ES involves the formation of a g-C_3N_4 coating layer on a silica optical fiber (SOF) surface coupled to a light-emitting diode (LED). The ATR-ES then interacts with MB adsorbed on the g-C_3N_4 interface to produce ATR-ES signal change. They have shown that, in the context of adsorption investigation using a red LED, the observed alteration in the "red" ATR-ES signified the spontaneous nature of the adsorption process. During the initial phase, rapid adsorption predominantly occurred due to electronic attraction. Subsequently, the slower adsorption was primarily driven by π–π interactions during the second phase. For the photodegradation, the change in the "violet" ATR-ES indicated that the adsorption–desorption equilibrium of MB was disrupted through oxidation by hydroxyl radicals (•OH) and superoxide radicals ($•O^{2-}$). Notably, the surface's apparent adsorption rate was 16 times higher than the apparent photodegradation rate constant. This discrepancy reveals that the photodegradation process is the primary rate-controlling step in the photocatalytic degradation reaction.

Finally, the feasibility of using the g-C_3N_4 composites in large-scale operations depends mainly on the material cost, disposal, and regeneration. The practical use of g-C_3N_4 composites for treating organic dyed wastewater needs to be improved by resolving the difficulties in separating and recovering the recycled sludge. Practices used most frequently, including filtration or centrifugation methods, are tedious, time-consuming, low-efficiency, and costly. Magnetically recoverable g-C_3N_4 composites by hybridizing with magnetic Fe_3O_4 or spinel ferrite (such as $NiFe_2O_4$) offer a promising means for easy recyclability and multiple reusable capabilities (Kumar et al., 2013; Guo et al., 2018; Sudhaik et al., 2018). Fixation of the g-C_3N_4 nanocomposite on mechanically robust and flexible filtration membranes, such as polyacrylonitrile porous substrates or carbon-fiber clothes, is another attractive alternative for resolving the regeneration issue in wastewater treatment (Lei et al., 2021; Li R. et al., 2019; Li X. et al., 2021). In addition, most of the studies are based on small-scale laboratory tests under reasonably well-controlled conditions. Scale-up research with testing conditions close to the actual situation is highly desirable to fill the knowledge gap for practical applications.

3. BN-based nanocomposites

BN is analogous to carbon in structure and consists of various crystalline polymorphs, including hexagonal form (h-BN) with honeycomb-like 2D layer structure together with rhombohedral (r-BN), cubic (c-BN), and wurtzite (w-BN) types with hybridized B–N bonds of either sp^2 or sp^3 types (Pakdel et al., 2014; Yu et al., 2018). The discovery of various carbon nanostructures, including fullerenes, nanowires, nanotubes, nanosheets, etc., has triggered the exploration of other nanostructured counterparts based on the similar honeycomb-like structure. The nanostructures include the layered graphene-like h-BN, with a wide range of nanostructures from 0D to 2D through synthesis methods such as exfoliation (mechanical or chemical), chemical vapor deposition, epitaxial growth, solid-state reaction, nanotube unzipping, or high-energy irradiation (Pakdel et al., 2014). Tuning the morphology of BN nanostructures gives rise to a unique combination of many advantageous properties, including high surface area, high-temperature oxidation resistance, high chemical inertness, possible low friction coefficient, high dielectric constant, tunable structural defect, and surface functionality. The morphological tunability renders BN nanostructures in wide-ranging potential applications, including electronic, optical, thermal, mechanical, wetting, and tribological uses. Depending on the atomic stacking configuration, the layered h-BN generally exhibits a considerable bandgap value of around 6 eV (Wickramaratne et al., 2018), prohibiting BN from being an efficient photocatalyst. However, BN-containing nanocomposites show a dual adsorptive and photocatalytic role. For example, AgI nanocomposites consisting of a minor addition of BN nanosheets have been shown to exhibit substantially enhanced photocatalytic activity and photocorrosion resistance, together with dye adsorption capability against aqueous RhB solutions under simulated sunlight irradiations when compared to pure AgI (Choi et al., 2015). BN–AgI heterojunction increases the charge transportation and separation efficiency for facilitating the photocatalytic degradation of RhB dyes. Similar synergistic findings have also been reported in the literature. As shown in **Table 5**, Wang et al. (2016) prepared porous h-BN fibers with their surface decorated by Ta_3N_5 nanoparticles of various fractions. The composite fibers showed preferential adsorption for selected dye molecules while facilitating the separation of photogenerated charge carriers.

In addition to the photocatalytic dye removal, porous BN nanosheets with high specific surface area, selective sorption capability, super-hydrophobicity, and facile regeneration have also received increasing attention as effective adsorbents in wastewater treatment (Lei et al., 2013; Park et al., 2022). For example, Liu et al. (2018) combined the adsorption advantage of BN and carbon by forming a highly porous, cheese-like 3D structure with pore sizes ranging from 2 nm to 100 nm. The BN/C composites showed a fast adsorption rate by removing cationic MB (>80 %) and anionic CR (>70 %) dyes in water (200 mL, 50 mg·L^{-1}) within merely ca. 5 min and over 95 % in 2 h duration. More importantly, the BN/C composites were reusable after heating in the air at 500 °C. After ten cycles of recycling, the reused composites maintained more than 70 % of their original adsorption capability. Recent advances in theoretical computations have revealed details about the adsorption process and molecular interactions between the adsorbent and adsorbate. Bangari et al. (2021) have used DFT calculations to examine the adsorption of MO dyes using BN nanosheets. Their results show that negative charge transfer occurred from MO to the nanosheets with high chemical potential. The finding suggests high chemical activity and a substantial decrease in the bandgap (up to 2.9 eV) after the adsorption. More importantly, theoretical computations have advanced to predict the simultaneous removal of multiple organic pollutants, including the adsorption affinity and adsorptive capacity, from the change of bandgap, geometrical bond distance, the molecular orientation of the adsorbate, adsorption energy, etc. (Bangari et al., 2022b; Yadav et al., 2022).

4. MXene-based nanocomposites

MXene belongs to the 2D materials family and finds enormous interest due to its proficient structural characteristics (e.g., large surface area, hydrophilic character, abundant active surface sites, etc.) and unique properties (e.g., high chemical stability, high electrical conductivity, quick

Table 5 Selected recent examples of BN nanocomposites for the adsorptive and/or photocatalytic dye removal in water treatment.

Composite	Dye	Light source	Dosage (mg)	Dye removal	Reference
BN/AgI	RhB (100 mL, 10 mg·L^{-1})	Simulated sun light (150 W Xe lamp with AM 1.5G filter)	100	ca. 60 %, 30 min by adsorption; >35 %, 70 min by photocatalysis	Choi et al., 2015
BN/Ta_3N_5	RhB, MB (100 mL, 50 mg·L^{-1})	300 W Xe lamp with 400 nm cutoff filter	50	ca. 20 %, 30 min by adsorption; >98 %, 120 min by photocatalysis	Wang et al., 2016
BN/C	MB, CR (200 mL, 50 mg·L^{-1})	Not used	100	>95 %, 120 min by adsorption	Liu et al., 2018
BN/Carbon nitride	Neutral red (NR), MG (30 mL, 200 mg·L^{-1})	Not used	5	1350.1 mg·g^{-1} (NR), 1040.6 mg·g^{-1} (MG) by adsorption	Guo et al., 2019
BN/polyvinyl alcohol foam	MB, CR, MO (6 mL, 25 mg·L^{-1})	Not used	N.A.	ca. 11.5, 5.1, 5.2 mg·g^{-1} for adsorption of MB, CR, MO, respectively	Gao et al., 2020
BN/TiO_2	RhB (20 mL, 10 mg·L^{-1})	300 W Xe lamp with 400 nm cutoff filter	15	95 %, 120 min by photocatalysis	Li et al., 2020
BN/SnO_2	MO (50 mL, 10 mg·L^{-1})	Visible light	1.25	92 %, ca. 7 min by photocatalysis	Singh et al., 2020
BN/chitosan/graphene	MB, Acid orange II	Simulated sun light	Up to 0.05	87 % (MB), 57 % (Acid orange II), 20 min by photocatalysis	Khose et al., 2021
BN/α-Fe_2O_3	MB (100 mL, 2.5 mg·L^{-1})	250 W tungsten-halogen lamp	10 or 20	ca. 91 %, 180 min by photocatalysis	Shenoy et al., 2021
BN/polyvinylidene fluoride	MB (150 ppm)	Not used	133*	100 % by membrane adsorption	Bangari et al., 2022a

N.A.: Not available. *: Estimated using 100 mL for the dyed solution.

ion-exchange capability, enriched surface functionality, environmentally benignity, etc.) (Naguib et al., 2014). The structure of MXene with a formula of $M_{n+1}X_nT_x$ (where n generally equals 1 to 3) consists of n+1 layers of transitional metal elements M, n layers of X (i.e., carbon and/or nitrogen), and a surface-terminal group of T_x (such as oxygen, fluorine, and hydroxyl) in periodic stacking configuration. The tunable surface termination renders MXene nanosheets potentially effective adsorbents for dyed wastewater treatment (Khandelwal and Darbha, 2021; Kumar et al., 2022; Rasool et al., 2019; Zhang et al., 2018). Mashtalir et al. first demonstrated preferential adsorption of $Ti_3C_2T_x$ for cationic MB dyes over anionic acid blue 80 in water primarily due to electrostatic interactions (Mashtalir et al., 2014). Interestingly, the photodegradation of both dyes occurred under UV light irradiation, revealing the instability of $Ti_3C_2T_x$ in water to form TiO_2 favorably for photocatalysis.

Table 6 lists examples of MXene composites using nitride for organic dye removal in wastewater remediation. All are g-C_3N_4 hybridized with MXene carbide of Ti_3C_2, showing enhanced photocatalytic dye degradation compared to the pure g-C_3N_4 counterpart. Although successful synthesis of MXene nitrides such as Ti_4N_3 (Urbankowski et al., 2016) and Ti_2N (Soundiraraju and George, 2017) has been reported, there has been no report on their use in the wastewater remediation to the author's best knowledge. Preparation of nitride MXene by selective acid etching from the MAX phase remains challenging and becomes one of the limiting factors for exploring its use in environmental water remediation.

5. Other nitride nanocomposites

Some other nitride-based nanocomposites are promising to become next-generation multi-purpose dye-removal solutions. For example, Tsai and Tseng recently prepared TiN–TiO_2 composite nanoparticles by a facile urea-glass route (Tsai and Tseng, 2020). The presence of TiN in the composites imparts a pronouncedly enhanced preferential adsorption against MB dyes in water in addition to their

Table 6 Selected recent examples of MXene nanocomposites using nitride for the adsorptive and/or photocatalytic dye removal in water treatment.

Composite	Dye	Light source	Dosage (mg)	Dye removal	Reference
Ti_3C_2/Ag/g-C_3N_4	RhB (200 mL, 10 mg·L^{-1})	300 W Xe lamp with 420 nm cutoff filter	100	ca. 20 %, 30 min by adsorption; 69.2 %, 70 min by photocatalysis	Huang et al., 2021
Ti_3C_2/g-C_3N_4	RhB (80 mL, 20 mg·L^{-1})	500 W metal halide lamp with 420 nm cutoff filter; 300 mW·cm^{-2}	40	ca. 99 %, 25 min by photocatalysis	Liu et al., 2022
Ti_3C_2/g-C_3N_4	MB (100 mL, 10 mg·L^{-1})	500 W halogen lamp	500	ca. 60 %, 180 min by photocatalysis	Nasri et al., 2022
Ti_3C_2-derived Ti-peroxo/g-C_3N_4	RhB (100 mL, 20 mg·L^{-1})	Visible light	20	ca. 55 %, 30 min by adsorption; 45 %, 110 min by photocatalysis	Tu et al., 2022

photocatalytic property under visible-light illuminations. The adsorption enhancement is directly proportional to the TiN fraction. Up to 95 % of the initial 10^{-5} M MB concentration can be removed by the adsorptive composites in less than 90 min. The composite particles show synergistic photocatalysis; in addition, niobium doping in the composite particles also facilitates dye removal, indicating that the creation of ionized defective sites may critically tune surface characteristics for adsorption and energy band offset at the interface for photocatalytic dye degradation.

A following report by Chen and Tseng revealed that TiN–WN composite nanoparticles also exhibit selective adsorption against cationic MB dyes in water. The adsorption under dark conditions reached as much as 90 % within 90 minutes when using an initial MB concentration of 10^{-5} M by tuning the TiN–WN composition. In comparison, virtually minimal adsorption (less than 10 %) resulted in the anionic MO dye solution under identical situations (Chen and Tseng, 2022). Similarly, the composite particles rendered a moderate photocatalytic degradation to the MB molecules under visible-light illuminations. Their results also suggest that the composite particles may be suitable for long-term wastewater treatment.

A recent finding further reveals that forming a $TiO_{2-x}N_x$ layer around Fe_3O_4@Ag core–shell nanoparticles is sufficient to impart preferential adsorption toward MB dyes in water (Lin and Tseng, 2022). By tuning the x value (x = 0.056 to 0.15) in the Fe_3O_4@Ag@$TiO_{2-x}N_x$ core–shell composite via the nitridation temperature, the composites with an x value of about 0.12 show dark adsorption of 54.8 % and an additional visible-light photodegradation of 25.1 % when using dyed wastewater with an initial MB concentration of 5×10^{-6} M. The composites with x about 0.15 can even exhibit dark adsorption of 99.1 % against the MB solution within 30 min, depending on the nitridation level. The nitrogen-dependent MB adsorption may involve multiple concurrent mechanisms, including the electrostatic interaction, formation of hydrogen bridges, electron donor–acceptor relationship, and the π–π electron dispersion force. In addition, the composite particles are magnetically responsive. The recycled particles retain over 72 % of their initial MB removal capability after five use cycles.

6. Summary and challenges

Nitride composites as a material group remain vastly unexplored for environmental remediation, despite intensive research endeavors devoted to wastewater treatment in the last decades. We have witnessed enormous groundbreaking advances in 2D nitrides (including g-C_3N_4, BN, and MXene) as an efficient photocatalyst through innovative synthesis, tailored morphological structure, bandgap engineering, optimal band alignment, defect tuning, etc. Many nitrides exhibit a strong affinity to adsorb specific dye attributes preferentially in a relatively short time. This dual role with synergistic dye-removal capability is pervasive among nitrides and is less common for other material counterparts. With the help of theoretical computations, we anticipate that the domain knowledge toward understanding the synergistic removal mechanism at the interface between nitride and dye molecules will advance at a faster speed in the coming future.

The effort to assess nitride composites' dye-removal performance in pilot-scale or field-scale experiments using actual wastewater samples is critically important to advance their practical use. So far, the practical use of nitride nanocomposites in large-scale wastewater treatment remains an unsurpassable hurdle to overcome. One must address pollutant-removal efficiency, scalability, long-term stability, cost-effectiveness, and regulatory consideration. To resolve this challenge, nitride composites with advantageous features such as reduced sludge formation, antifouling capability, facile recycle operation, and multiple regeneration usability are highly desirable. Developing effective dye-removal systems that integrate the nitride

composites into existing wastewater-treatment processes may provide a viable route for practical application. The transition from laboratory research to practical implementation in large-scale industrial or municipal wastewater treatment can be complex. The challenges may foster innovative new ideas and become opportunities in the near future.

Conflict of Interest

The author declares no known competing financial interests or personal relationships that could have appeared to influence the work reported in this paper.

Acknowledgments

Financial support from the National Science and Technology Council (NSTC) of Taiwan under contract numbers 110-2221-E-005-015-MY3 and 110-2221-E-005-016-MY3 is gratefully acknowledged. Assistance from the Taiwan Instrument Research Institute is much appreciated.

Credit Author Statement

W.J. Tseng contributed to conceptualization, literature search, data curation, writing, reviewing, editing, and funding acquisition.

Data Availability Statement

Available upon reasonable request.

References

Acharya R., Parida K., A review on TiO_2/g-C_3N_4 visible-light-responsive photocatalysts for sustainable energy generation and environmental remediation, J. Environ. Chem. Eng., 8 (2020) 103896. https://doi.org/10.1016/j.jece.2020.103896

Adegoke A.A., Amoah I.D., Stenström T.A., Verbyla M.E., Mihelcic J.R., Epidemiological evidence and health risks associated with agricultural reuse of partially treated and untreated wastewater: a review, Front. Public Health, 6 (2018) 337. https://doi.org/10.3389/fpubh.2018.00337

Ahmadi A., Hajilou M., Zavari S., Yaghmaei S., A comparative review on adsorption and photocatalytic degradation of classified dyes with metal/non-metal-based modification of graphitic carbon nitride nanocomposites: Synthesis, mechanism, and affecting parameters, J. Clean. Prod., 382 (2023) 134967. https://doi.org/10.1016/j.jclepro.2022.134967

Al-Tohamy R., Ali S.S., Li F., Okasha K.M., Mahmoud Y.A.-G., Elsamahy T., Jiao H., Fu Y., Sun J., A critical review on the treatment of dye-containing wastewater: ecotoxicological and health concerns of textile dyes and possible remediation approaches for environmental safety, Ecotoxicol. Environ. Saf., 231 (2022) 113160. https://doi.org/10.1016/j.ecoenv.2021.113160

Aspera S.M., David M., Kasai H., First-principles study of the adsorption of water on tri-s-triazine-based graphitic carbon nitride, Jap. J. Appl. Phys., 49 (2010) 115703. https://doi.org/10.1143/JJAP.49.115703

Bangari R.S., Yadav A., Sinha N., Experimental and theoretical investigations of methyl orange adsorption using boron nitride nanosheets, Soft Matter, 17 (2021) 2640–2651. https://doi.org/10.1039/d1sm00048a

Bangari R.S., Yadav A., Bharadwaj J., Sinha N., Boron nitride nanosheets incorporated polyvinylidene fluoride mixed matrix membranes for removal of methylene blue from aqueous stream, J. Environ. Chem. Eng., 10 (2022a) 107052. https://doi.org/10.1016/j.jece.2021.107052

Bangari R.S., Yadav A., Awasthi P., Sinha N., Experimental and theoretical analysis of simultaneous removal of methylene blue and tetracycline using boron nitride nanosheets as adsorbent, Colloid. Surf. A, 634 (2022b) 127943. https://doi.org/10.1016/j.colsurfa.2021.127943

Chandel N., Sharma K., Sudhaik A., Raizada P., Hosseini-Bandegharaei A., Thakur V.K., Singh P., Magnetically separable ZnO/$ZnFe_2O_4$ and ZnO/$CoFe_2O_4$ photocatalysts supported onto nitrogen doped graphene for photocatalytic degradation of toxic dyes, Arab. J. Chem., 13 (2020) 4324–4340. https://doi.org/10.1016/j.arabjc.2019.08.005

Chen C.-Y., Tseng W.J., Preparation of TiN-WN composite particles for selective adsorption of methylene blue dyes in water, Adv. Powder Technol., 33 (2022) 103423. https://doi.org/10.1016/j.apt.2021.103423

Chen Z., Zhang S., Liu Y., Alharbi N.S., Rabah S.O., Wang S., Wang X., Synthesis and fabrication of g-C_3N_4-based materials and their application in elimination of pollutants, Sci. Total Environ., 731 (2020) 139054. https://doi.org/10.1016/j.scitotenv.2020.139054

Choi J., Reddy D.A., Kim T.K., Enhanced photocatalytic activity and anti-photocorrosion of AgI nanostructures by coupling with graphene-analogue boron nitride nanosheets, Ceram. Int., 41 (2015) 13793–13803. https://doi.org/10.1016/j.ceramint.2015.08.062

Choudri B.S., Charabi Y., Health effects associated with wastewater treatment, reuse, and disposal, Water Environ. Res., 91 (2019) 976–983. https://doi.org/10.1002/wer.1157

Connor R., The United Nations World Water Development Report 2015: Water for a Sustainable World (Vol. 1), UNESCO Publishing, 2015. ISBN 978-92-3-100071-3.

Cui Y., Ding Z., Liu P., Antonietti M., Fu X., Wang X., Metal-free activation of H_2O_2 by g-C_3N_4 under visible light irradiation for the degradation of organic pollutants, Phys. Chem. Chem. Phys., 14 (2012) 1455–1462. https://doi.org/10.1039/c1cp22820j

Darkwah W.K., Ao Y., Mini review on the structure and properties (photocatalysis), and preparation techniques of graphitic carbon nitride nano-based particle, and Its applications, Nanoscale Res. Lett., 13 (2018) 388. https://doi.org/10.1186/s11671-018-2702-3

Degano I., Ribechini E., Modugno F., Colombini M.P., Analytical methods for the characterization of organic dyes in artworks and in historical textiles, Appl. Spectrosc. Rev., 44 (2009) 363–410. https://doi.org/10.1080/05704920902937876

Di J., Xia J., Yin S., Xu H., Xu L., Xu Y., He M., Li H., Preparation of sphere-like g-C_3N_4/BiOI photocatalysts via a reactable ionic liquid for visible-light-driven photocatalytic degradation of pollutants, J. Mater. Chem. A, 2014, 2, 5340–5351. https://doi.org/10.1039/c3ta14617k

Dickin S.K., Schuster-Wallace C.J., Qadir M., Pizzacalla K., A review of health risks and pathways for exposure to wastewater use in agriculture, Environ. Health Perspect., 124 (2016) 900–909. https://doi.org/10.1289/ehp.1509995

Ding C., Kang S., Li W., Gao W., Zhang Z., Zheng L., Cui L., Mesoporous structure and amorphous Fe-N sites regulation in Fe-g-C_3N_4 for boosted visible-light-driven photo-Fenton reaction, J. Colloid Interf. Sci., 608 (2022) 2515–2528. https://doi.org/10.1016/j.jcis.2021.10.168

Dong G., Zhang Y., Pan Q., Qiu J., A fantastic graphitic carbon nitride (g-C_3N_4) material: electronic structure, photocatalytic and photoelectronic properties, J. Photochem. Photobiol. C, 20 (2014) 33–50. https://doi.org/10.1016/j.jphotochemrev.2014.04.002

Forgacs E., Cserháti T., Oros G., Removal of synthetic dyes from wastewaters: a review, Environ. Int., 30 (2004) 953–971. https://doi.org/10.1016/j.envint.2004.02.001

Fronczak M., Adsorption performance of graphitic carbon nitride-based materials: current state of the art, J. Environ. Chem. Eng., 8 (2020) 104411. https://doi.org/10.1016/j.jece.2020.104411

Gao X., Li R., Hu L., Lin J., Wang Z., Yu C., Fang Y., Gao X., Li R., Hu L., Lin J., Wang Z., Yu C., Fang Y., Preparation of boron nitride nanofibers/PVA composite foam for environmental remediation, Colloid. Surf. A, 604 (2020) 125287. https://doi.org/10.1016/j.colsurfa.2020.125287

Ghanbari M., Salavati-Niasari M., Copper iodide decorated graphitic

carbon nitride sheets with enhanced visible-light response for photocatalytic organic pollutant removal and antibacterial activities, Ecotoxicol. Environ. Saf., 208 (2021) 111712. https://doi.org/10.1016/j.ecoenv.2020.111712

Groenewolt M., Antonietti M., Synthesis of g-C_3N_4 nanoparticles in mesoporous silica host matrices, Adv. Mater., 17 (2005) 1789–1792. https://doi.org/10.1002/adma.200401756

Guo F., Lu J., Liu Q., Zhang P., Zhang A., Cai Y., Wang Q., Degradation of acid orange 7 by peroxymonosulfate activated with the recyclable nanocomposites of g-C_3N_4 modified magnetic carbon, Chemosphere 205 (2018) 297–307. https://doi.org/10.1016/j.chemosphere.2018.04.139 0045-6535

Guo Y., Wang R., Wang P., Rao L., Wang C., Developing a novel layered boron nitride−carbon nitride composite with high efficiency and selectivity to remove protonated dyes from water, ACS Sustain. Chem. Eng. 2019, 7, 5727–5741. https://doi.org/10.1021/acssuschemeng.8b05150

Hamidian A.H., Ozumchelouei E.J., Feizi F., Wu C., Zhang Y., Yang M., A review on the characteristics of microplastics in wastewater treatment plants: a source for toxic chemicals, J. Clean. Prod., 295 (2021) 126480. https://doi.org/10.1016/j.jclepro.2021.126480

He Y., Zhang L., Fan M., Wang X., Walbridge M.L., Nong Q., Wu Y., Zhao L., Z-scheme SnO_{2-x}/g-C_3N_4 composite as an efficient photocatalyst for dye degradation and photocatalytic CO_2 reduction, Sol. Energy Mater. Sol. Cells, 137 (2015) 175–184. https://doi.org/10.1016/j.solmat.2015.01.037

Hu C., Lin Y.-R., Yang H.-C., Recent developments in graphitic carbon nitride based hydrogels as photocatalysts, ChemSusChem, 12 (2019) 1794–1806. https://doi.org/10.1002/cssc.v12.9

Huang K., Li C., Wang L., Wang W., Meng X., Layered Ti_3C_2 MXene and silver co-modified g-C_3N_4 with enhanced visible light-driven photocatalytic activity, Chem. Eng. J., 425 (2021) 131493. https://doi.org/10.1016/j.cej.2021.131493

Huang L., Xu H., Li Y., Li H., Cheng X., Xia J., Xu Y., Cai G., Visible-light-induced WO_3/g-C_3N_4 composites with enhanced photocatalytic activity, Dalton Trans., 42 (2013) 8606–8616. https://doi.org/10.1039/c3dt00115f

Iqbal S., Ahmad N., Javed M., Qamar M.A., Bahadur A., Ali S., Ahmad Z., Irfan R.M., Liu G., Akbar M.B., Qayyum M.A., Designing highly potential photocatalytic comprising silver deposited ZnO NPs with sulfurized graphitic carbon nitride (Ag/ZnO/S-g-C_3N_4) ternary composite, J. Environ. Chem. Eng., 9 (2021) 104919. https://doi.org/10.1016/j.jece.2020.104919

Islam A, Teo S.H., Taufiq-Yap Y.H., Ng C.H., Vo D.-V.N., Ibrahim M.L., Hasan M.M., Khan M.A.R., Nur A.S.M., Awual M.R., Step towards the sustainable toxic dyes removal and recycling from aqueous solution—A comprehensive review, Resour. Conserv. Recycl., 175 (2021) 105849. https://doi.org/10.1016/j.resconrec.2021.105849

Ismael M., Wu Y., Taffa D.H., Bottke P., Wark M., Graphitic carbon nitride synthesized by simple pyrolysis: the role of the precursor on the photocatalytic hydrogen production, New J. Chem., 43 (2019) 6909–6920. https://doi.org/10.1039/C9NJ00859D

Jiang L., Yuan X., Pan Y., Liang J., Zeng G., Wu Z., Wang H., Doping of graphitic carbon nitride for photocatalysis: a review, Appl. Catal. B: Environ., 217 (2017) 388–406. https://doi.org/10.1016/j.apcatb.2017.06.003

Jo W.-K., Tonda S., Novel CoAl-LDH/g-C_3N_4/RGO ternary heterojunction with notable 2D/2D/2D configuration for highly efficient visible-light-induced photocatalytic elimination of dye and antibiotic pollutants, J. Hazard. Mater., 368 (2019) 778–787. https://doi.org/10.1016/j.jhazmat.2019.01.114

Khandelwal N., Darbha G.K., A decade of exploring MXenes as aquatic cleaners: covering a broad range of contaminants, current challenges and future trends, Chemosphere, 279 (2021) 130587. https://doi.org/10.1016/j.chemosphere.2021.130587

Khose R.V., Lokhande K.D., Bhakare M.A., Dhumal P.S., Wadekar P.H., Some S., Boron nitride doped chitosan functionalized graphene for an efficient dye degradation, ChemistrySelect, 6 (2021) 7956–7963. https://doi.org/10.1002/slct.202101611

Kudo A, Miseki Y., Heterogeneous photocatalyst materials for water splitting, Chem. Soc. Rev., 38 (2009) 253–278. https://doi.org/10.1039/b800489g

Kumar J.A., Prakash P., Krithiga T., Amarnath D.J., Premkumar J., Rajamohan N., Vasseghian Y., Saravanan P.y, Rajasimman M., Methods of synthesis, characteristics, and environmental applications of MXene: a comprehensive review, Chemosphere, 286 (2022) 131607. https://doi.org/10.1016/j.chemosphere.2021.131607

Kumar S., T. Surendar, Kumar B., Baruah A., Shanker V., Synthesis of magnetically separable and recyclable g-C_3N_4–Fe_3O_4 hybrid nanocomposites with enhanced photocatalytic performance under visible-light irradiation, J. Phys. Chem. C, 117 (2013) 26135–26143. https://doi.org/10.1021/jp409651g

Lam S.-M., Sin J.-C., Mohamed A.R., A review on photocatalytic application of g-C_3N_4/semiconductor (CNS) nanocomposites towards the erasure of dyeing wastewater, Mater. Sci. Semicond. Process., 47 (2016) 62–84. https://doi.org/10.1016/j.mssp.2016.02.019

Lapointe B.E., Herren L.W., Debortoli D.D., Vogel M.A., Evidence of sewage-driven eutrophication and harmful algal blooms in Florida's Indian River Lagoon, Harmful Algae, 43 (2015) 82–102. https://doi.org/10.1016/j.hal.2015.01.004

Lei L., Wang W., Wang C., Zhang M., Zhong Q., Fan H., In situ growth of boron doped g-C_3N_4 on carbon fiber cloth as a recycled flexible film-photocatalyst, Ceram. Int., 47 (2021) 1258–1267. https://doi.org/10.1016/j.ceramint.2020.08.246

Lei W., Portehault D., Liu D., Qin S., Chen Y., Porous boron nitride nanosheets for effective water cleaning, Nature Commun., 4 (2013) 1777. https://doi.org/10.1038/ncomms2818

Lellis B., Fávaro-Polonio C.Z., Pamphile J.A., Polonio J.C., Effects of textile dyes on health and the environment and bioremediation potential of living organisms, Biotechnol. Res. Innov., 3 (2019) 275–290. https://doi.org/10.1016/j.biori.2019.09.001

Li F., Yu Z., Shi H., Yang Q., Chen Q., Pan Y., Zeng G., Yan L., A Mussel-inspired method to fabricate reduced graphene oxide/g-C_3N_4 composites membranes for catalytic decomposition and oil-in-water emulsion separation, Chem. Eng. J., 322 (2017) 33–45. https://doi.org/10.1016/j.cej.2017.03.145

Li H., Tu W., Zhou Y., Zou Z., Z-Scheme photocatalytic systems for promoting photocatalytic performance: recent progress and future challenges, Adv. Sci., (2016) 1500389. https://doi.org/10.1002/advs.201500389

Li Q., Hou X., Fang Z., Yang T., Chen J., Cui X., Liang T., Shi J., Construction of layered h-BN/TiO_2 hetero-structure and probing of the synergetic photocatalytic effect, Sci. China Mater., 63 (2020) 276–287. https://doi.org/10.1007/s40843-019-1180-8

Li R., Ren Y., Zhao P., Wang J., Liu J., Zhang Y., Graphitic carbon nitride (g-C_3N_4) nanosheets functionalized composite membrane with self-cleaning and antibacterial performance, J. Hazard. Mater., 365 (2019) 606–614. https://doi.org/10.1016/j.jhazmat.2018.11.033

Li X., Huang G., Chen X., Huang J., Li M., Yin J., Liang Y., Yao Y., Li Y., A review on graphitic carbon nitride (g-C_3N_4) based hybrid membranes for water and wastewater treatment, Sci. Total Environ., 792 (2021) 148462. https://doi.org/10.1016/j.scitotenv.2021.148462

Lin Y.-H., Tseng W.J., Multifunctional Fe_3O_4@Ag@$TiO_{2-x}N_x$ core-shell composite particles for dye adsorption and visible-light photocatalysis, Ceram. Int., 48 (2022) 13906–13913. https://doi.org/10.1016/j.ceramint.2022.01.275

Liu D., Li C., Ge J., Zhao C., Zhao Q., Zhang F., Ni T., Wu W., 3D interconnected g-C_3N_4 hybridized with 2D Ti_3C_2 MXene nanosheets for enhancing visible light photocatalytic hydrogen evolution and dye contaminant elimination, Appl. Surf. Sci., 579 (2022) 152180. https://doi.org/10.1016/j.apsusc.2021.152180

Liu Z., Fang Y., Jia H., Wang C., Song Q., Li L., Lin J., Huang Y., Yu C., Tang C., Novel multifunctional cheese-like 3D carbon-BN as a highly efficient adsorbent for water purification, Sci. Rep., 8 (2018) 1104. https://doi.org/10.1038/s41598-018-19541-5

Lu X., Xu K., Chen P., Jia K., Liu S., Wu C., Facile one step method realizing scalable production of g-C_3N_4 nanosheets and study of their photocatalytic H_2 evolution activity, J. Mater. Chem. A, 2 (2014) 18924–18928. https://doi.org/10.1039/c4ta04487h

Luo Y., Zhu Y., Han Y., Ye H., Liu R., Lan Y., Xue M., Xie X., Yu S.,

Zhang L., Yin Z., Gao B., g-C_3N_4-based photocatalysts for organic pollutant removal: acritical review, Carbon Res., 2 (2023) 14. https://doi.org/10.1007/s44246-023-00045-5

Ma J., Yang Q., Wen Y., Liu W., Fe-g-C_3N_4/graphitized mesoporous carbon composite as an effective Fenton-like catalyst in a wide pH range, Appl. Catal. B, 201 (2017) 232–240. https://doi.org/10.1016/j.apcatb.2016.08.048

Market Analysis Report, Dyes and pigments market size, share & trends analysis report by product (dyes (reactive, vat, acid, direct, disperse), pigment (organic, inorganic)), by application, by region, and segment forecasts, 2023–2030, Grand View Research, (2023) Report ID: GVR-1-68038-545-8.

Martıńez-Huitle C.A., Brillas E., Decontamination of wastewaters containing synthetic organic dyes by electrochemical methods: a general review, Appl. Catal. B – Environ. 87 (2009) 105–145. https://doi.org/10.1016/j.apcatb.2008.09.017

Mashtalir O., Cook K.M., Mochalin V.N., Crowe M., Barsoum M.W., Gogotsi Y., Dye adsorption and decomposition on two-dimensional titanium carbide in aqueous media, J. Mater. Chem. A, 2 (2014) 14334–14338. https://doi.org/10.1039/c4ta02638a

Meng S., Nan Z., Rapid and selective adsorption of organic dyes with ultrahigh adsorption capacity using Na and Fe co-doped g-C_3N_4, Sep. Purif. Technol., 297 (2022) 121420. https://doi.org/10.1016/j.seppur.2022.121420

Modwi A., Khezami L., Ghoniem M.G., Nguyen-Tri P., Baaloudj O., Guesmi A., AlGethami F.K., Amer M.S., Assadi A.A., Superior removal of dyes by mesoporous MgO/g-C_3N_4 fabricated through ultrasound method: adsorption mechanism and process modeling, Environ. Res., 205 (2022) 112543. https://doi.org/10.1016/j.envres.2021.112543

Monga D., Ilager D., Shetti N.P., Basu S., Aminabhavi T.M., 2D/2d heterojunction of MoS_2/g-C_3N_4 nanoflowers for enhanced visible-light-driven photocatalytic and electrochemical degradation of organic pollutants, J. Environ. Manage., 274 (2020) 111208. https://doi.org/10.1016/j.jenvman.2020.111208

Naguib M., Mochalin V.N., Barsoum M.W., Gogotsi Y., MXenes: a new family of two-dimensional materials, Adv. Mater., 26 (2014) 992–1005. https://doi.org/10.1002/adma.201304138

Nasri M.S.I., Samsudin M.F.R., Tahir A.A., Sufian S., Effect of MXene loaded on g-C_3N_4 photocatalyst for the photocatalytic degradation of methylene blue, Energies, 15 (2022) 955. https://doi.org/10.3390/en15030955

Nnadiekwe C.C., Mustapha U., Abdulazeez I., Alhooshani K., Al-Saadi A.A., Alkali metal ion-doped heptazine-based g-C_3N_4 quantum dots for efficient adsorption of methyl blue: a DFT perspective, Surf. Interf., 38 (2023) 102852. https://doi.org/10.1016/j.surfin.2023.102852

Park Y.-G., Nam S.-N., Jang M., Park C.M., Her N., Sohn J., Cho J., Yoon Y., Boron nitride-based nanomaterials as adsorbents in water: a review, Sep. Purif. Technol., 288 (2022) 120637. https://doi.org/10.1016/j.seppur.2022.120637

Pakdel A., Bando Y., Golberg D., Nano boron nitride flatland, Chem. Soc. Rev., 43 (2014) 934–959. https://doi.org/10.1039/c3cs60260e

Preisner M., Neverova-Dziopak E., Kowalewski Z., Analysis of eutrophication potential of municipal wastewater, Water Sci. Technol., 81 (2020) 1994–2003. https://doi.org/10.2166/wst.2020.254

Preisner M., Neverova-Dziopak E., Kowalewski Z., Mitigation of eutrophication caused by wastewater discharge: a simulation-based approach, Ambio, 50 (2021) 413–424. https://doi.org/10.1007/s13280-020-01346-4

Qamar M.A., Shahid S., Javed M., Iqbal S., Sher M., Bahadur A., AL-Anazy M.M., Laref A., Li D., Designing of highly active g-C_3N_4/Ni-ZnO photocatalyst nanocomposite for the disinfection and degradation of the organic dye under sunlight radiations, Colloids Surf., 614 (2021) 126176. https://doi.org/10.1016/j.colsurfa.2021.126176

Qin S., Xiong Y., Li J., Wan H., Fang S., Duan M., Li R., Liao D., Real-time adsorption and photodegradation investigation of dye removal on g-C_3N_4 surface by attenuated total reflectance induced evanescent spectroscopy, J. Phys. Chem. C, 125 (2021) 4027–4040. https://doi.org/10.1021/acs.jpcc.0c11482

Raizada P., Thakur P., Sudhaik A., Singh P., Thakur V.K., Hosseini-Bandegharaei A., Fabrication of dual Z-scheme photocatalyst via coupling of BiOBr/Ag/AgCl heterojunction with P and S co-doped g-C_3N_4 for efficient phenol degradation, Arab. J. Chem., 13 (2020) 4538–4552. https://doi.org/10.1016/j.arabjc.2019.10.001

Rasool K., Pandey R.P., Rasheed P.A., Buczek S., Gogotsi Y., Mahmoud K.A., Water treatment and environmental remediation applications of two-dimensional metal carbides (MXenes), Mater. Today, 30 (2019) 80–102. https://doi.org/10.1016/j.mattod.2019.05.017

Santoso E., Ediati R., Kusumawati Y., Bahruji H., Sulistiono D.O., Prasetyoko D., Review on recent advances of carbon based adsorbent for methylene blue removal from waste water, Mater. Today Chem., 16 (2020) 100233. https://doi.org/10.1016/j.mtchem.2019.100233

Saravanan A., Kumar P.S., Jeevanantham S., Karishma S., Tajsabreen B., Yaashikaa P.R., Reshma B., Effective water/wastewater treatment methodologies for toxic pollutants removal: processes and applications towards sustainable development, Chemosphere, 280 (2021) 130595. https://doi.org/10.1016/j.chemosphere.2021.130595

Shen L., Xing Z., Zou J., Li Z., Wu X., Zhang Y., Zhu Q., Yang S., Zhou W., Black TiO_2 nanobelts/g-C_3N_4 nanosheets laminated heterojunctions with efficient visible-light-driven photocatalytic performance, Sci. Rep., 7 (2017) 41978. https://doi.org/10.1038/srep41978

Shenoy M.R., Ayyasamy S., Bhojan V., Swaminathan R., Raju N., Kumar P.S., Sasikumar M., Kadarkarai G., Tamilarasan S., Thangavelu S., Suryakanth J., Reddy M.V., Visible light sensitive hexagonal boron nitride (hBN) decorated Fe_2O_3 photocatalyst for the degradation of methylene blue, J. Mater. Sci. Mater. Electron., 32 (2021) 4766–4783. https://doi.org/10.1007/s10854-020-05215-4

Sher M., Javed M., Shahid S., Iqbal S., Qamar M.A., Bahadur A., Qayyum M.A., The controlled synthesis of g-C_3N_4/Cd-doped ZnO nanocomposites as potential photocatalysts for the disinfection and degradation of organic pollutants under visible light irradiation, RSC Adv., 11 (2021) 2025–2039. https://doi.org/10.1039/d0ra08573a

Shi W., Ren H., Huang X., Li M., Tang Y., Guo F., Low cost red mud modified graphitic carbon nitride for the removal of organic pollutants in wastewater by the synergistic effect of adsorption and photocatalysis, Sep. Purif. Technol., 237 (2020) 116477. https://doi.org/10.1016/j.seppur.2019.116477

Singh B., Singh K., Kumar M., Thakur S., Kumar A., Insights of preferred growth, elemental and morphological properties of BN/SnO_2 composite for photocatalytic applications towards organic pollutants, Chem. Phys., 531 (2020) 110659. https://doi.org/10.1016/j.chemphys.2019.110659

Singh K., Arora S., Removal of synthetic textile dyes from wastewaters: a critical review on present treatment technologies, Crit. Rev. Environ. Sci. Technol., 41 (2011) 807–878. https://doi.org/10.1080/10643380903218376

Soundiraraju B., George B.K., Two-dimensional titanium nitride (Ti_2N) MXene: synthesis, characterization, and potential application as surface-enhanced Raman scattering substrate, ACS Nano, 11 (2017) 8892–8900. https://doi.org/10.1021/acsnano.7b03129

Sudhaik A., Raizada P., Shandilya P., Singh P., Magnetically recoverable graphitic carbon nitride and $NiFe_2O_4$ based magnetic photocatalyst for degradation of oxytetracycline antibiotic in simulated wastewater under solar light, J. Environ. Chem. Eng., 6 (2018) 3874–3883. https://doi.org/10.1016/j.jece.2018.05.039

Teter D.M., Hemley R.J., Low-compressibility carbon nitrides, Science, 271 (1996) 53–55. https://doi.org/10.1126/science.271.5245.53

Thomas A., Fischer A., Goettmann F., Antonietti M., Müller J.-O., Schlögl R., Carlsson J.M., Graphitic carbon nitride materials: variation of structure and morphology and their use as metal-free catalysts, J. Mater. Chem., 18 (2008) 4893–4908. https://doi.org/10.1039/b800274f

Tian Y., Zhang J., Wang W., Liu J., Zheng X., Li J., Guan X., Facile assembly and excellent elimination behavior of porous BiOBr-g-C_3N_4 heterojunctions for organic pollutants, Environ. Res., 209 (2022) 112889. https://doi.org/10.1016/j.envres.2022.112889

Tsai C.-G., Tseng W.J., Preparation of TiN–TiO_2 composite nanoparticles for organic dye adsorption and photocatalysis, Ceram. Int., 46 (2020) 14529–14535. https://doi.org/10.1016/j.ceramint.2020.02.252

Tu W., Liu Y., Chen M., Zhou Y., Xie Z., Ma L., Li L., Yang B., Carbon nitride coupled with Ti_3C_2-Mxene derived amorphous Ti-peroxo heterojunction for photocatalytic degradation of rhodamine B and tetracycline, Colloid. Surf. A, 640 (2022) 128448. https://doi.org/10.1016/j.colsurfa.2022.128448

Urbankowski P., Anasori B., Makaryan T., Er D., Kota S., Walsh P.L., Zhao M., Shenoy V.B., Barsouma M.W., Gogotsi Y., Synthesis of two-dimensional titanium nitride Ti_4N_3 (MXene), Nanoscale, 8 (2016) 11385–11391. https://doi.org/10.1039/c6nr02253g

Wang A., Wang C., Fu L., Wong-Ng W., Lan Y., Recent advances of graphitic carbon nitride-based structures and applications in catalyst, sensing, imaging, and LEDs, Nano-Micro Lett., 9 (2017) 47. https://doi.org/10.1007/s40820-017-0148-2

Wang Q., Wang W., Zhong L., Liu D., Cao X., Cui F., Oxygen vacancy-rich 2D/2D BiOCl-g-C_3N_4 ultrathin heterostructure nanosheets for enhanced visible-light-driven photocatalytic activity in environmental remediation, Appl. Catalys. B: Environ., 220 (2018) 290–302. https://doi.org/10.1016/j.apcatb.2017.08.049

Wang Q., Zhang L., Guo Y., Shen M., Wang M., Li B., Shi J., Multifunctional 2D porous g-C_3N_4 nanosheets hybridized with 3D hierarchical TiO_2 microflowers for selective dye adsorption, antibiotic degradation and CO_2 reduction, Chem. Eng. J., 396 (2020) 125347. https://doi.org/10.1016/j.cej.2020.125347

Wang S., Luo H., Xu X., Bai Y., Song X., Zhang J., Li J., Zhao J., Tang C., Enhanced organic dye removal of porous BN fibers supported Ta_3N_5 nanoparticles under visible light irradiation, Surf. Interf., 5 (2016) 39–46. https://doi.org/10.1016/j.surfin.2016.10.001

Wang X., Maeda K., Chen X., Takanabe K., Domen K., Hou Y., Fu X., Antonietti M., Polymer semiconductors for artificial photosynthesis: hydrogen evolution by mesoporous graphitic carbon nitride with visible light, J. Am. Chem. Soc., 131 (2009) 1680–1681. https://doi.org/10.1021/ja809307s

Wei Y., Zhu Y., Jiang Y., Photocatalytic self-cleaning carbon nitride nanotube intercalated reduced graphene oxide membranes for enhanced water purification, Chem. Eng. J., 356 (2019) 915–925. https://doi.org/10.1016/j.cej.2018.09.108

Wickramaratne D., Weston L., Van de Walle C.G., Monolayer to bulk properties of hexagonal boron nitride, J. Phys. Chem. C, 122 (2018) 25524–25529. https://doi.org/10.1021/acs.jpcc.8b09087

Xu B, Ahmed M.B., Zhou J.L., Altaee A., Xu G., Wu M., Graphitic carbon nitride based nanocomposites for the photocatalysis of organic contaminants under visible irradiation: progress, limitations and future directions, Sci. Total Environ., 633 (2018) 546–559. https://doi.org/10.1016/j.scitotenv.2018.03.206

Xu Q., Zhang L., Cheng B., Fan J., Yu J., S-scheme heterojunction photocatalyst, Chem, 6 (2020) 1543–1559. https://doi.org/10.1016/j.chempr.2020.06.010

Yadav A., Dindorkar S.S., Ramisetti S.B., Sinh N., Simultaneous adsorption of methylene blue and arsenic on graphene, boron nitride and boron carbon nitride nanosheets: Insights from molecular simulations, J. Water Proc. Eng., 46 (2022) 102653. https://doi.org/10.1016/j.jwpe.2022.102653

Yagub M.T., Sen T.K., Afroze S., Ang H.M., Dye and its removal from aqueous solution by adsorption: a review, Adv. Colloid Interf. Sci., 209 (2014) 172–184. https://doi.org/10.1016/j.cis.2014.04.002

Yan H., Soft-templating synthesis of mesoporous graphitic carbon nitride with enhanced photocatalytic H_2 evolution under visible light, Chem. Commun., 48 (2012) 3430–3432. https://doi.org/10.1039/c2cc00001f

Yaseen D.A., Scholz M., Textile dye wastewater characteristics and constituents of synthetic effluents: a critical review, Int. J. Environ. Sci. Technol., 16 (2019) 1193–1226. https://doi.org/10.1007/s13762-018-2130-z

Yu J., Wang S., Low J., Xiao W., Enhanced photocatalytic performance of direct Z-scheme g-C_3N_4/TiO_2 photocatalyst for decomposition of formaldehyde in air, Phys. Chem. Chem. Phys., 15 (2013) 16883–16890. https://doi.org/10.1039/C3CP53131G

Yu S., Wang X., Pang H., Zhang R., Song W., Fu D., Hayat T., Wang X., Boron nitride-based materials for the removal of pollutants from aqueous solutions: a review, Chem. Eng. J., 333 (2018) 343–360. https://doi.org/10.1016/j.cej.2017.09.163

Zhan B., Liu Y., Zhou W.-T., Li S.-Y., Chen Z.-B., Stegmaier T., Aliabadi M., Han Z.-W., Ren L.-Q., Multifunctional 3D GO/g-C_3N_4/TiO_2 foam for oil-water separation and dye adsorption, Appl. Surf. Sci., 541 (2021) 148638. https://doi.org/10.1016/j.apsusc.2020.148638

Zhang L., Zhang J., Yu H., Yu J., Emerging S-scheme photocatalyst, Adv. Mater., 34 (2022) 2107668. https://doi.org/10.1002/adma.202107668

Zhang Y., Wang L., Zhang N., Zhou Z., Adsorptive environmental applications of MXene nanomaterials: a review, RSC Adv., 8 (2018) 19895–19905. https://doi.org/10.1039/c8ra03077d

Zhao G.-Q., Zou J., Hu J., Long X., Jiao F.-P., A critical review on graphitic carbon nitride (g-C_3N_4)-based composites for environmental remediation, Sep. Purif. Technol., 279 (2021) 119769. https://doi.org/10.1016/j.seppur.2021.119769

Zhao Z., Sun Y, Dong F., Graphitic carbon nitride based nanocomposites: a review, Nanoscale, 7 (2015) 15–37. https://doi.org/10.1039/c4nr03008g

Zhao Z., Ma Y., Fan J., Xue Y., Chang H., Masubuchi Y., Yin S., Synthesis of graphitic carbon nitride from different precursors by fractional thermal polymerization method and their visible light induced photocatalytic activities, J. Alloys Compd., 735 (2018) 1297–1305. https://doi.org/10.1016/j.jallcom.2017.11.033

Zhu B., Xia P., Ho W., Yu J., Isoelectric point and adsorption activity of porous g-C_3N_4, Appl. Surf. Sci., 344 (2015) 188–195. https://doi.org/10.1016/j.apsusc.2015.03.086

Zhu J., Xiao P., Li H., Carabineiro S.A.C., Graphitic carbon nitride: synthesis, properties, and applications in catalysis, ACS Appl. Mater. Interf., 6 (2014) 16449–16465. https://doi.org/10.1021/am502925j

Zollinger H., Color Chemistry: Syntheses, Properties, and Applications of Organic Dyes and Pigments, Third Edition, Wiley VCH 2003, ISBN: 9783906390239.

Author's Short Biography

Prof. Wenjea J. Tseng is a Distinguished Professor in the Materials Science and Engineering Department of the National Chung Hsing University. He graduated with a diploma in Metallurgy from the National Taipei Institute of Technology, Taiwan, and his M.S. and Ph.D. degrees in Materials Science from the University of Rochester, New York, U.S.A. His research interests include colloidal processing of fine particles, chemical synthesis of functionalized nanostructures, organic-inorganic hybrid materials, photocatalysis, and gas sensing. He has published more than 100 technical papers and holds over 10 patents. He served as a council member and committee commissioner for the Taiwan Ceramic Society.